ADSORPTION OF CYTOSINE ON A MERCURY ELECTRODE

Dorota SIEŃKO[1], Jolanta NIESZPOREK[2], Krzysztof NIESZPOREK[3], Dorota GUGAŁA[4] and Jadwiga SABA[5,*]

Faculty of Chemistry, Maria Curie-Skłodowska University, 20-031 Lublin, Poland;
e-mail: [1] dsienko@hermes.umcs.lublin.pl, [2] jolan@hermes.umcs.lublin.pl,
[3] krzysn@hektor.umcs.lublin.pl, [4] gugala@hermes.umcs.lublin.pl, [5] jsaba@hermes.umcs.lublin.pl

Received February 17, 2006
Accepted May 26, 2006

The electrosorption behavior of cytosine at the mercury electrode/acetic buffer of pH 4 and 5 interfaces was determined from the double-layer differential capacity measurements extrapolated to zero frequency. Solutions of cytosine were prepared to cover the range from 1×10^{-4} to 6×10^{-3} mol dm^{-3}. Adsorption of cytosine was described by the adsorption isotherms constants derived from the surface pressure data as a function of electrode charge density and bulk concentration. The obtained values of the relative surface excesses Γ' were higher in the acetic buffer of pH 4 than of pH 5. Maximum of cytosine adsorption in the mentioned buffers was at –581 and –551 mV, respectively. The values of the standard Gibbs energy $\Delta G°$ obtained from the Frumkin isotherm were higher in the buffer of pH 4 than of pH 5. The values of the interaction parameter A indicated weaker repulsive interaction between adsorbed molecules of cytosine in the former buffer. The adsorption parameters obtained from the virial isotherm confirmed corresponding parameters obtained from the Frumkin isotherm. The dependences of Φ^{M-2} on the relative surface excess at a constant charge density were analyzed in order to calculate the electrostatic parameters of the inner layer.

Keywords: Cytosine; Mercury; Differential capacity; Adsorption isotherms; Electrostatic parameters; Electrochemistry.

Cytosine is the base compound of nucleosides and nucleotides, ubiquitous constituents of the living cells. The study of its adsorption on the mercury/water interface could be interesting in relation to their activity in biological interfaces. In living cells, nucleic acids come into contact with various types of boundaries. The surfaces of mammalian cells and other biological membranes carry an appreciable electrical potential. The electric double-layer formed in the immediate vicinity of a charged membrane–biological fluid interface may be regarded as essentially identical to that formed at an electrode surface–electrolyte solution interface[1]. Adsorption of uracil and thymine – derivatives of pyrimidine – have been extensively studied[2–22].

doi:10.1135/cccc20061393

Adsorptive two-dimensional condensation layers of cytosine are widely described in literature[23–37]. However, information about the adsorption of the cytosine from dilute solutions is scarcer. Adsorption study of this aromatic molecule with a high dipole moment located in the ring structure could bring out interesting information about the role played by the electrostatic and the electronic interactions with the metal. The paper is a part of complex studies of the influence of adsorption layer with the use of pyrimidine derivatives on the kinetics and mechanism of Zn^{2+} ions electroreduction[38]. Acetic buffers of pH 4 and 5 were used in these studies to prevent the hydrolysis of Zn^{2+} ions. In the present study, the double-layer capacitance is chosen as the primary experimental quantity. Adsorption of cytosine is described by the adsorption isotherm constants derived from the surface pressure data as a function of electrode charge density and bulk concentration.

EXPERIMENTAL

Analytical grade reagents: cytosine (Sigma), CH_3COOH and CH_3COONa (Fluka) were used without any purification. Water and mercury were double-distilled before use. The solutions were deaerated by high-purity nitrogen. Nitrogen was also passed over the solution during the measurements, which were carried out at 298 ± 0.1 K. Ten different concentrations of cytosine in the range from 1×10^{-4} to 6×10^{-3} mol dm^{-3} were prepared dissolving a known amount of cytosine in a definite volume of acetic buffer of pH 4 or 5. This range of cytosine concentrations do not refer to concentrations where two-dimensional condensation layers are formed. Measurements were carried using a three-electrode cell consisting of a dropping mercury electrode as a working electrode, an Ag|AgCl|saturated NaCl as a reference electrode, and a platinum spiral as a counter-electrode. A controlled-growth mercury drop-electrode (CGMDE) manufactured by MTM, Poland was used. The reference electrode was connected to the electrolytic cell via an intermediate vessel filled with the base solution of acetic buffer of pH 4 or 5. The double-layer capacity (C) was measured using the ac impedance technique with the Autolab frequency response analyzer (Eco Chemie BV, Netherlands). The reproducibility of the average capacity measurements was ±0.5%. The measurements were carried out at several frequencies with amplitude of 5 mV. The potentials of zero charge, E_z, were measured using a streaming mercury electrode. The interfacial tensions, γ_z, were measured by the maximum-bubble pressure method following Schiffrin[39], after calibration with 0.05 mol dm^{-3} Na_2SO_4, and taking the maximum value of interfacial tension as 426.2 mN m^{-1} (ref.[40]). The charge density and surface tension of cytosine were derived by the back-integration of differential capacity–potential dependences. No corrections for the effects of the medium on the activity of the supporting electrolyte[41,42] and activity coefficient of the adsorbate[43] were made.

RESULTS AND DISCUSSION

Analysis of Experimental Data

The differential capacity curves obtained at several frequencies in the range of 200–2000 Hz indicate distinct frequency dispersion (Fig. 1). The extrapolation was carried out by plotting the measured capacity against the square root of the frequency to the zero frequency. This procedure assumes that the impedance of the double-layer is equivalent to a series capacity–resistance combination, and the rate of adsorption is diffusion-controlled.

The differential capacity curves extrapolated to zero frequency (Figs 2 and 3) are typical of aromatic compounds with lack of the adsorption–desorption peaks at positive charges. The negative potential range accessible for a thermodynamic analysis is limited by the reduction of cytosine, so only those potentials at which the in-phase component of the cell impedance does not show any contribution of the faradaic process have been considered.

Generally, changes of differential capacity in the absence as well as in the presence of cytosine are more distinct in the acetic buffer of pH 5 than of

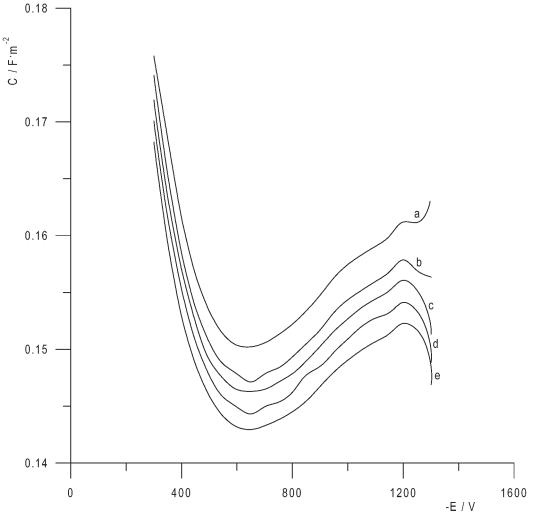

FIG. 1

Frequency dispersion (in Hz) of differential capacity–potential curves of the mercury electrode in contact with acetic buffer of pH 4 containing 6×10^{-3} M cytosine: a 200, b 400, c 800, d 1200, e 2000

pH 4. In both the systems, lowest concentrations of cytosine increase the differential capacity compared with the base electrolyte. This effect could be a result of the competitive adsorption in the studied systems and changes of physical interactions of CH_3COOH molecules on mercury surface into specific interactions of aromatic ring of cytosine molecules. Higher concentrations of cytosine ($c \geq 7.5 \times 10^{-4}$ mol dm^{-3}) decrease the differential capacity at less negative potentials while at more negative potentials a rise in capacity occurs. As not all of the obtained *C–E* curves converge at sufficiently negative potentials with the corresponding curve for the base solution, the capacities against the potential data were numerically integrated from the point of E_z. The relevant E_z and γ_z values are presented in Table I.

It can be noted that the value of E_z in acetic buffer of pH 4 without cytosine is shifted to a less negative potential in comparison with acetic buffer of pH 5. This is the result of greater concentration of acetic acid in the first buffer and stronger adsorption of acetic acid molecules placed with the positive end on the mercury surface. An introduction of cytosine into the base solutions causes a shift of E_z values to less negative potentials, which con-

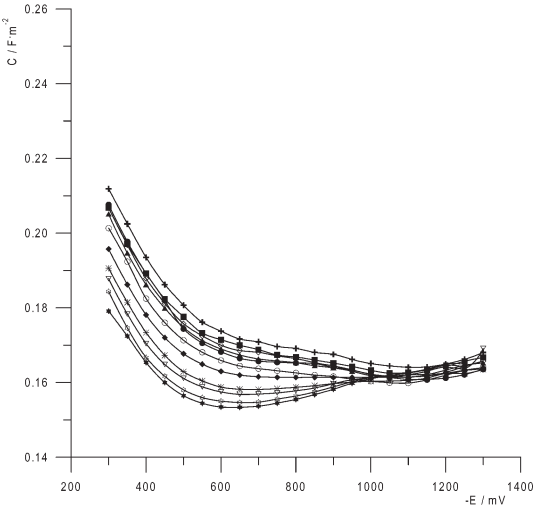

FIG. 2

Differential capacity–potential curves of the mercury electrode in contact with acetic buffer of pH 4 (●) containing different concentrations of cytosine (in mol dm^{-3}): ✚ 1.0×10^{-4}, ◇ 2.5×10^{-4}, ■ 5.0×10^{-4}, ▲ 7.5×10^{-4}, ○ 1.0×10^{-3}, ◆ 2.0×10^{-3}, ❋ 3.0×10^{-3}, ▽ 4.0×10^{-3}, ✡ 5×10^{-3}, ✶ 6.0×10^{-3}

TABLE I
Potentials of zero charge $-E_z$ (in mV) vs Ag|AgCl and surface tensions γ_z (in mN m^{-1}) for E_z in the acetate buffers containing various amounts of cytosine

$c_{cytosine} \times 10^{-3}$ mol dm^{-3}	pH 4		pH 5	
	$-E_Z$, mV	γ_Z, mN m^{-1}	$-E_Z$, mV	γ_Z, mN m^{-1}
0.00	411.2	417.0	416.3	419.8
0.10	410.3	416.1	415.2	417.6
0.25	409.1	415.2	414.4	413.4
0.50	405.9	414.4	412.2	407.1
0.75	403.3	413.5	411.9	396.1
1.00	402.0	411.7	410.5	392.1
2.00	396.4	410.7	400.1	377.9
3.00	392.3	410.4	397.9	372.4
4.00	388.0	410.0	395.8	367.9
5.00	385.1	402.2	391.2	362.3
6.00	383.2	407.4	383.7	360.6

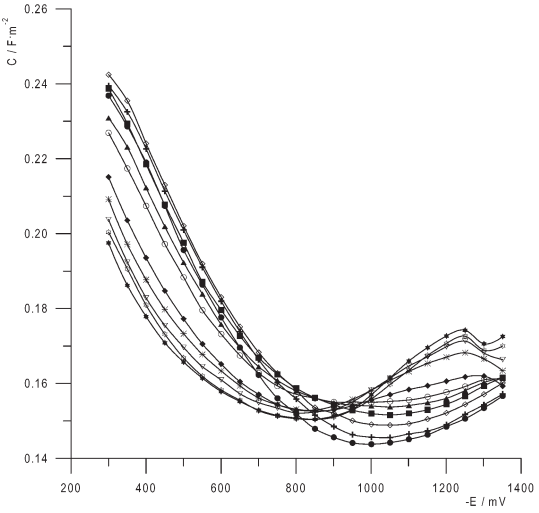

FIG. 3
Differential capacity–potential curves of the mercury electrode in contact with acetic buffer of pH 5 (●) containing different concentrations of cytosine (in mol dm^{-3}): ✚ 1.0×10^{-4}, ◇ 2.5×10^{-4}, ■ 5.0×10^{-4}, ▲ 7.5×10^{-4}, ○ 1.0×10^{-3}, ◆ 2.0×10^{-3}, ❋ 3.0×10^{-3}, ▽ 4.0×10^{-3}, ✡ 5×10^{-3}, ✶ 6.0×10^{-3}

firm that cytosine dipole molecules are placed with its positive end on the mercury electrode. A greater shift of E_z values in buffer of pH 5 and a stronger decrease in γ_z values could indicate stronger adsorption of cytosine in this buffer. The data obtained from the integration of differential capacity curves were subsequently used to calculate Parson's auxiliary function $\xi = \gamma + \sigma E$, where σ is the electrode charge and E is the electrode potential. The obtained σ–E curves at different concentrations of cytosine intersect at a point, with the coordinates of maximum adsorption, independent of the concentration[44]. The values were: E_{max} = –581.0 and –551.0 mV while σ_{max} = –3.0 and –2.7 μC cm^{-2} in the acetic buffer of pH 4 and 5, respectively. As the adsorption of the base electrolyte was obvious, adsorption of cytosine was described using the relative surface excess, which according to the Gibbs adsorption isotherm is given by:

$$\Gamma' = \frac{1}{RT}\left[\frac{\partial \Phi}{\partial \ln c}\right]_{\sigma} \qquad (1)$$

where c is the bulk concentration of cytosine and Φ is the surface pressure: $\Phi = \Delta\xi = \xi_0 - \xi$ (ξ_0 and ξ are the values of Parson's auxiliary functions for base electrolyte and for the solution containing cytosine, respectively).

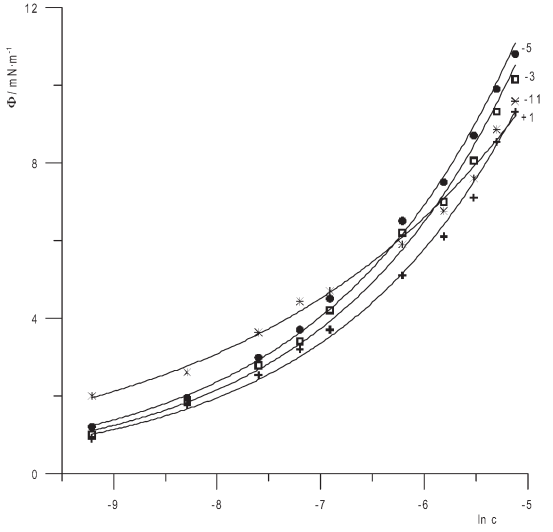

FIG. 4
Surface pressure as a function of the bulk concentration of cytosine in acetic buffer of pH 4, electrode charges (σ in 10^{-2} C m^{-2}) indicated by each curve

Figure 4 shows plots of Φ vs ln c_{cytosine} for acetic buffer of pH 4 and selected electrode charges. The values of Γ' obtained for this system depending on surface charge and cytosine concentration are presented in Fig. 5.

Generally, the values of Γ' are markedly higher (by ca. 50%) in acetic buffer of pH 4 in comparison with acetic buffer of pH 5. All Γ'–σ curves show a maximum which coincides with the $\sigma_{\max}$ obtained from σ–E curves. The shape of curves in Fig. 5 shows competitive electrostatic interactions: organic molecules–water dipoles[45]. The obtained Γ' values do not confirm the conclusion derived from values of E_z and γ_z. This fact can be caused by the difference in the level of cytosine protonation as well as in different levels of hydration of the electrode surface in both the buffers used. Such effects can decide about the dynamics of competitive adsorption in the system: H_2O–CH_3COOH–CH_3COO^-–cytosine. Surface excess tends towards a limit when concentration is increased at each charge. The surface excess at saturation, Γ_s was estimated by extrapolating the $1/\Gamma'$ versus $1/c$ at different charges to $1/c \rightarrow 0$. In acetic buffer of pH 4 the value of Γ_s was 2.0×10^{-6} mol m^{-2} and in acetic buffer of pH 5 it was 3.3×10^{-6} mol m^{-2}, while Γ_s for uracil in 0.5 M NaF is 2.61×10^{-6} mol m^{-2} (ref.[21]). The corresponding

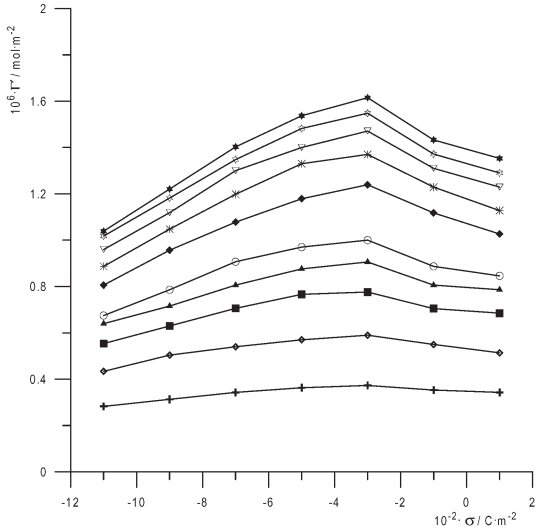

FIG. 5

Relative surface excess of cytosine as a function of the electrode charge (σ in 10^{-2} C m^{-2}) and the bulk concentration of cytosine (in mol dm^{-3}) in acetic buffer of pH 4: ✚ 1.0×10^{-4}, ◇ 2.5×10^{-4}, ■ 5.0×10^{-4}, ▲ 7.5×10^{-4}, ○ 1.0×10^{-3}, ◆ 2.0×10^{-3}, ❋ 3.0×10^{-3}, ▽ 4.0×10^{-3}, ✡ 5×10^{-3}, ✶ 6.0×10^{-3}

values of the surface occupied by one cytosine molecule ($S = 1/N\Gamma_s$, where N is Avogadro number) were 0.83 and 0.50 nm^2. The value 0.83 nm^2 indicates a planar orientation of cytosine molecule on the electrode surface and an influence of the acetic acid presence on the electrode surface in buffer of pH 4.

Adsorption Isotherms

The adsorption of cytosine was further analyzed on the basis of the constants obtained from the Frumkin isotherm:

$$\beta x = \left(\frac{\Theta}{1-\Theta}\right)\exp(-2A\Theta) \qquad (2)$$

where x is the mole fraction of cytosine in solution, β is the adsorption coefficient: $\beta = \exp(-\Delta G°/RT)$, $\Delta G°$ is the standard Gibbs energy of adsorption, A is the interaction parameter and Θ is the coverage ($\Theta = \Gamma'/\Gamma_s$). Figure 6 presents the linear test of the Frumkin isotherm for the acetic buffer of pH 4.

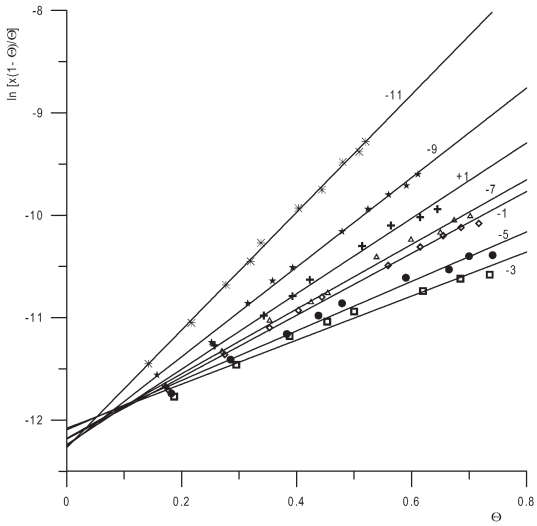

FIG. 6
Linear test of the Frumkin isotherm for the system acetic buffer of pH 4–cytosine, electrode charges (σ in 10^{-2} C m^{-2}) indicated by each line

The values of the parameter *A* were calculated from the slopes of the lines on the linear test of the Frumkin isotherm, and the corresponding values of ΔG_F^o were determined by the extrapolation of the lines of ln $[(1 - \Theta)x/\Theta]$ vs Θ to the value $\Theta = 0$. The values of ΔG_F^o for the range of σ between +1 and –11 μC cm^{-2} change from –30.4 to –29.9 kJ mol^{-1} and from –29.6 to –27.3 kJ mol^{-1} in the acetic buffer of pH 4 and 5, respectively. The corresponding values of the parameter *A* change from –2.9 to –1.1 and from –6.7 to –4.2 (Fig. 7).

Higher values of Γ' in the buffer of pH 4 are the result of corresponding higher values of ΔG_F^o and weaker repulsive interaction between adsorbed molecules of cytosine. As the values of Γ_s for cytosine vary significantly in the used buffers, the virial isotherm (which does not need the knowledge of the value of Γ_s) was used in the description of cytosine adsorption:

$$\ln \beta c = \ln \Gamma + 2B\Gamma \qquad (3)$$

where *B* is two-dimensional (2D) second virial coefficient. Figure 8 shows the linear test of the virial isotherm for the acetic buffer of pH 4–cytosine system.

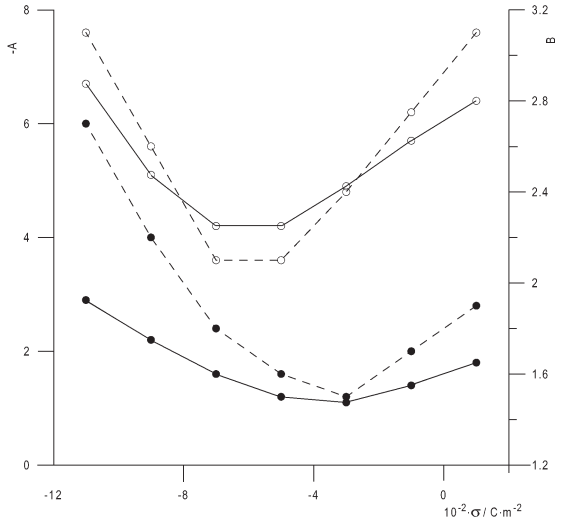

FIG. 7
Interaction parameter *A* (——) and second virial coefficient *B* (- - - -) as a function of electrode charge in acetic buffer of pH 4 (●) and pH 5 (○)

Values of 2D second virial coefficient were calculated from the slopes of lines in Fig. 8 and the corresponding ΔG_V^o values were obtained from the intercepts of these lines with the axis $\log(\Gamma'/c)$ using the standard state 1 mol dm^{-3} in the bulk solution and 1 mol cm^{-2} on the surface. The obtained values of coefficient *B* confirm the changes of *A* parameter values (Fig. 7). In the buffer of pH 4 the ΔG_V^o value is independent from electrode charge and equals –106.7 kJ mol^{-1}. In the second studied buffer the ΔG_V^o is –107.1 kJ mol^{-1} for $\sigma \geq -3$ μC m^{-2} and –105.1 kJ mol^{-1} for $\sigma \leq -3$ μC m^{-2}. The obtained values of $\Delta G°$ confirm stronger adsorption of cytosine in comparison with uracil and its derivatives[22].

Electrostatic Parameters of the Inner Layer

According to the Parson's electrostatic model the potential drop across the inner layer Φ^{M-2} at the constant charge can be represented by the sum:

$$\Phi^{M-2} = \frac{4\pi\sigma}{\varepsilon_i} x_2 + \frac{4\pi\mu}{\varepsilon_i} \Gamma' \qquad (4)$$

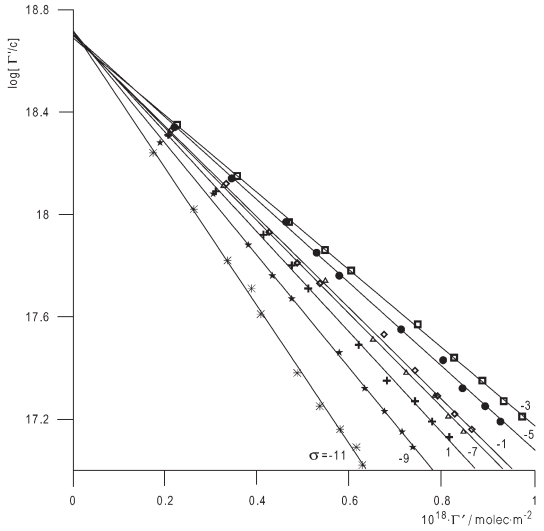

FIG. 8
Linear test of the virial isotherm for the system acetic buffer of pH 4–cytosine, electrode charges (σ in 10^{-2} C m^{-2}) indicated by each line

where μ is the dipole moment of an isolated cytosine molecule (μ = 21.6 × 10^{-30} C m)[46], ε_i is the permittivity of the inner layer and x_2 is the inner layer thickness. The inner layer parameters, i.e. ε_i, x_2 and the integral capacity values K^i were determined in terms of this model. The value of $\Phi^{M-2} = E - E_z - \Phi^{2-s}$, where E is the measured potential for a given concentration of cytosine, E_z is the potential of zero charge in the absence of cytosine, and Φ^{2-s} is the potential drop across the diffuse layer, which can be calculated using the Gouy–Chapman theory. The dependence of Φ^{M-2} on the Γ' at a constant charge density for buffer of pH 4 is presented in Fig. 9.

It can be seen from Fig. 9 that the changes in potential drop across the inner layer are linear. The linearity of the plots Φ^{M-2} vs Γ' at a constant σ is a further evidence that the adsorption of cytosine can be described by an isotherm congruent in electrode charge. In the buffer of pH 5, the changes of Φ^{M-2} vs Γ' are non-linear (Fig. 10). The observed effect can result from the fact that addition of organic molecules to an electrolyte solution often effectively raises the activity of the salt[32]. It should be noted that the concentration of CH_3COOH is ten-fold lower in the buffer of pH 5 than of pH 4.

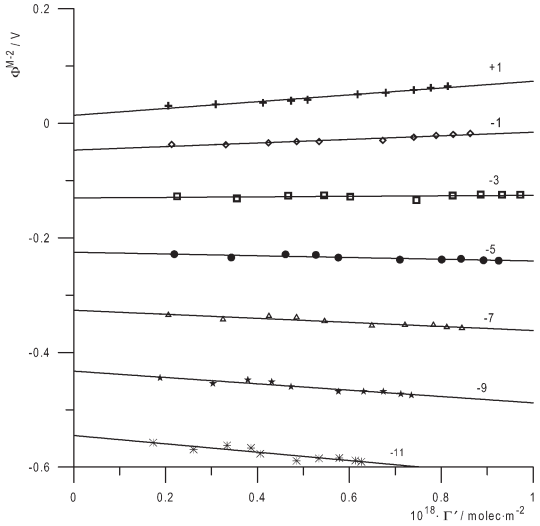

FIG. 9

Potential drop across the inner layer as a function of the cytosine amount adsorbed in acetic buffer of pH 4, at constant electrode charges (σ in 10^{-2} C m^{-2}) indicated by each line

TABLE II

Inner layer properties for cytosine adsorbed at the mercury|water–acetic buffer system interface; σ (in 10^{-2} C m^{-2}), K^i (in 10^{-2} F m^{-2}), x_2 (in nm)

σ_1 / 10^{-2} C m^{-2}	pH 4			pH 5		
	ε_i	K^i, 10^{-2} F m^{-2}	x_2, nm	ε_i	K^i, 10^{-2} F m^{-2}	x_2, nm
–3	81.2	18.9	3.80	79.9	12.5	5.66
–5	122.2	18.9	5.73	30.5	11.1	2.43
–7	81.2	18.9	3.80	26.9	9.4	2.52
–9	60.9	18.9	2.86	20.3	6.3	2.84
–11	30.5	18.9	1.43	17.5	4.6	3.37

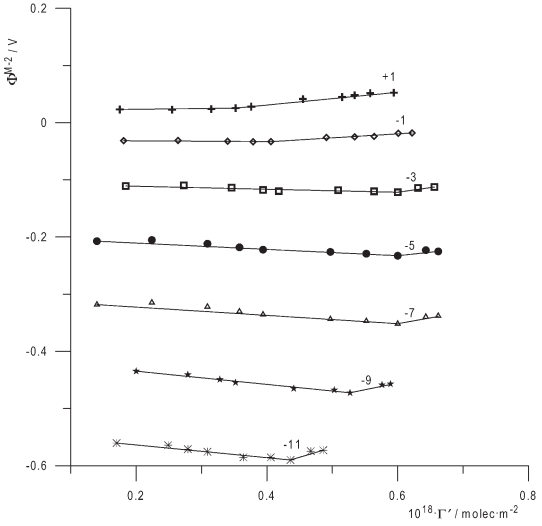

FIG. 10

Potential drop across the inner layer as a function of the cytosine amount adsorbed in acetic buffer of pH 5, at constant electrode charges (σ in 10^{-2} C m^{-2}) indicated by each line

The cause of non-linearity in Fig. 10 may also be due to a change in the orientation of the adsorbed cytosine molecules from flat at lower values of Γ′ to skew at higher values of Γ′, which also indicate changes in *A* parameters, greater in buffer of pH 5 in comparison with buffer of pH 4. The rectilinear segments in Fig. 10 obtained for smaller values of Γ′ were analyzed in a way similar to that used previously by Jurkiewicz-Herbich and Jastrzębska[47]. The obtained inner layer parameters (Table II) depend insignificantly on Γ′. This may be the result of dominant influence of the base electrolyte on the structure of the inner layer. Additionally, the K^i value is independent of σ values.

The obtained values of K^i appear to be reasonable whereas ε_i values are too high and, in consequence, values of x_2 are also too high. The values of the electrostatic parameters of the inner layer calculated on the basis of a simple electrostatic model of inner potential distribution are not correct in all cases, indicating that a simple electrostatic model is not fully applicable to the description of the systems studied in this work, at negative values of electrode charge density.

REFERENCES

1. Pilla A. A.: *Bioelectrochem. Bioenerg.* **1974**, *1*, 227.
2. Sridharan R., De Levie R.: *J. Electroanal. Chem.* **1986**, *201*, 133.
3. Srinivasan R., De Levie R.: *J. Electroanal. Chem.* **1986**, *201*, 145.
4. Saffarian M. H., Sridharan R., De Levie R.: *J. Electroanal. Chem.* **1987**, *218*, 273.
5. Wandlowski T., Kretschmer E., Müller E., Kuschel F., Hoffmann S., Lipiński K. J.: *J. Electroanal. Chem.* **1986**, *213*, 339.
6. Wandlowski T., Pospíšil L.: *J. Electroanal. Chem.* **1989**, *258*, 179.
7. Wandlowski T., Pospíšil L.: *J. Electroanal. Chem.* **1989**, *270*, 319.
8. Wandlowski T.: *J. Electroanal. Chem.* **1991**, *302*, 233.
9. Wandlowski T.: *J. Electroanal. Chem.* **1990**, *293*, 219.
10. De Levie R., Wandlowski T.: *J. Electroanal. Chem.* **1994**, *366*, 265.
11. Nikitas P., Pappa-Louisi A.: *J. Electroanal. Chem.* **1993**, *346*, 483.
12. Kim M. H., Christian S. D., Dryhurst G.: *J. Electroanal. Chem.* **1979**, *104*, 165.
13. Sowerby S. J., Petersen G. B.: *J. Electroanal. Chem.* **1997**, *433*, 85.
14. Roelfs R., Bunge E., Schröter C., Solomun T., Meyer H., Nichols R. J., Baumgärtel H.: *J. Phys. Chem. B* **1997**, *101*, 754.
15. Popov A., Naneva R., Dimitrov N., Vitanov T., Bostanov V., De Levie R.: *Electrochim. Acta* **1992**, *37*, 2369.
16. Popov A., Dimitrov N., Vitanov T.: *Electrochim. Acta* **1992**, *37*, 2373.
17. Hölzle M. H., Krznarić D., Kolb D. M.: *J. Electroanal. Chem.* **1995**, *386*, 235.
18. Kinoshita H., Christian S. D., Dryhurst G.: *J. Electroanal. Chem.* **1977**, *85*, 377.
19. Brabec V., Christian S. D., Dryhurst G.: *J. Electroanal. Chem.* **1977**, *85*, 389.
20. Brabec V., Christian S. D., Dryhurst G.: *Biophys. Chem.* **1978**, *7*, 253.

21. Kamal M. M., Ahmed Z. A., Ahmed M. E., Ibrahim M. S., Temerk Y. M.: *Bioelectrochem. Bioenerg.* **1991**, *25*, 137.
22. Brabec V., Christian S. D., Dryhurst G.: *Biophys. Chem.* **1978**, *8*, 151.
23. Vetterl V., Papadopoulos N., Dražan V., Strašák L., Hasoň S., Dvořák J.: *Electrochim. Acta* **2000**, *45*, 2961.
24. Yamada T., Shirasaka K., Takanao A., Kawai M.: *Surf. Sci.* **2004**, *561*, 233.
25. Vetterl V.: *Collect. Czech. Chem. Commun.* **1966**, *31*, 2105.
26. Webb J., Janik B., Elving P. J.: *J. Am. Chem. Soc.* **1973**, *95*, 991.
27. Chen E. S. D., Chen E. C. M., Sane N., Shulze S.: *Bioelectrochem. Bioenerg.* **1999**, *48*, 69.
28. Vetterl V.: *Experientia* **1965**, *21*, 9.
29. Vetterl V.: *Bioelectrochem. Bioenerg.* **1976**, *3*, 338.
30. Retter U.: *J. Electroanal. Chem.* **1980**, *106*, 371.
31. Vetterl V., Pokorný J.: *Bioelectrochem. Bioenerg.* **1980**, *7*, 517.
32. Jursa J., Vetterl V.: *Bioelectrochem. Bioenerg.* **1984**, *12*, 137.
33. Jursa J., Vetterl V.: *Studia Biophys.* **1986**, *114*, 75.
34. Šponer J., Leszczyński J., Vetterl V., Hobza P.: *J. Biomol. Struct. Dyn.* **1996**, *13*, 695.
35. Brabec V., Vetterl V., Vrána O. in: *Bioelectrochemistry: Principles and Practice* (G. Milazzo, Ed.), Vol. 3, p. 287. Birghäuser Verlag, Basel 1996.
36. Paleček E., Fojta M., Jelen F., Vetterl V. in: *Encyclopedia of Electrochemistry* (A. J. Bard and M. Stratman, Eds), *Bioelectrochemistry* (G. S. Wilson, Ed.), Vol. 9, p. 265. Wiley–VCH Verlag, Weinheim 2002.
37. Vetterl V., Hasoň S. in: *Perspectives in Bioanalysis* (E. Paleček, F. Scheller and J. Wang, Eds), Vol. 1, p. 18. Elsevier Ltd., London 2005.
38. Nieszporek J., Gugała D., Sieńko D., Szaran J., Saba J.: *Electrochim. Acta* **2006**, *51*, 2278.
39. Schiffrin D. J.: *J. Electroanal. Chem.* **1969**, *23*, 168.
40. Smolders C. C., Duyvies E. M.: *Rec. Trav. Chim. Pays-Bas* **1961**, *80*, 636.
41. Battisti A. D., Trasatti S.: *J. Electroanal. Chem.* **1974**, *54*, 1.
42. Mohilner D. M., Nakadomari H.: *J. Phys. Chem.* **1973**, *77*, 1594.
43. Mohilner D. M., Browman L. W., Freeland S. J., Nakadomari H.: *J. Electrochem. Soc.* **1973**, *120*, 1658.
44. Trasatti S., Olivieri G.: *J. Electroanal. Chem.* **1970**, *27*, App. 7.
45. Schapink F. W., Oudeman M., Leu K. W., Helle J. N.: *Trans. Faraday Soc.* **1960**, *56*, 415.
46. Schiedt J., Weinkauf R., Neumark D. M., Schlag E. W.: *Chem. Phys.* **1998**, *239*, 511.
47. Jurkiewicz-Herbich M., Jastrzębska J.: *Pol. J. Chem.* **1984**, *58*, 1125.